PROCEEDINGS OF SCIENCE

An update on the determination of the sphaleron rate in finite temperature QCD

Nicolò Bellini,[a,b] **Claudio Bonanno,**[c] **Francesco D'Angelo,**[a,b,d,*] **Massimo D'Elia,**[a,b] **Andrea Giorgieri**[a,b] **and Lorenzo Maio**[e,f]

[a] *Università di Pisa, Largo B. Pontecorvo 3, I-56127 Pisa, Italy*

[b] *INFN, Sezione di Pisa, Largo B. Pontecorvo 3, I-56127 Pisa, Italy*

[c] *Instituto de Física Teórica UAM-CSIC, c/ Nicolás Cabrera 13-15, Universidad Autónoma de Madrid, Cantoblanco, E-28049 Madrid, Spain*

[d] *INFN, Sezione di Roma Tre, Via della Vasca Navale 84, I-00146 Rome, Italy*

[e] *Aix Marseille Univ., Université de Toulon, CNRS, CPT, Marseille 13009, France*

[f] *Dipartimento di Fisica, Università di Roma "Tor Vergata" and INFN, Sezione di Roma Tor Vergata, Via della Ricerca Scientifica 1, I-00133 Rome, Italy*

E-mail: francesco.dangelo@phd.unipi.it

The sphaleron rate is a key phenomenological quantity both for the axion thermal production in the Early Universe and the Chiral Magnetic Effect occurring in the Quark-Gluon Plasma in presence of a background magnetic field. In this talk we present an extension of our recent determination of the sphaleron rate, in the SU(3) gauge theory, based on the determination of the two-point function of the topological charge density at finite temperature.

The 41st International Symposium on Lattice Field Theory (LATTICE2024)
28 July - 3 August 2024
Liverpool, UK

*Speaker

PoS(LATTICE2024)198

1. Introduction

The study of real time QCD topological transitions at finite temperature, described by the *strong sphalerons*, is extremely important not only for a better understanding of the QCD vacuum properties, but also for their phenomenological implications. The relevant physical quantity that describes these thermal processes is the *strong sphaleron rate*, defined as

$$\Gamma_{\rm Sphal} = \lim_{\substack{V_s\to\infty \\ t_{\rm M}\to\infty}} \frac{1}{V_s t_{\rm M}} \left\langle \left[\int_0^{t_{\rm M}} dt'_{\rm M} \int_{V_s} d^3x\, q(t'_{\rm M},\vec{x}) \right]^2 \right\rangle = \int dt_{\rm M} d^3x \, \langle q(t_{\rm M},\vec{x}) q(0,\vec{0}) \rangle \,, \tag{1}$$

where $t_{\rm M}$ is the Minkowskian time and

$$q(x) = \frac{1}{32\pi^2} \epsilon_{\mu\nu\rho\sigma} \, {\rm Tr}\{G^{\mu\nu}(x) G^{\rho\sigma}(x)\} \tag{2}$$

is the topological charge density operator, with $G_{\mu\nu}$ being the gauge field strength.

The strong sphaleron rate plays an important phenomenological role in different contexts such as Quark-Gluon Plasma (QGP) and axion physics. For instance, a non vanishing $\Gamma_{\rm Sphal}$ is related to local imbalances in the number of left/right-handed quark species in the QGP, giving rise to the well-known Chiral Magnetic Effect [1–4], i.e., the appearance of an electric current in the same direction of a background magnetic field. On the other side, as pointed out in a recent paper [5], this quantity is also related to the thermal production of axions in the Early Universe, as it enters the Boltzmann equation for the 3-momentum dependent axion distribution function.

Since sphaleron dynamics is strictly non-perturbative, the lattice regularization provides a useful framework for the determination of $\Gamma_{\rm Sphal}$. However, Monte Carlo simulations on the lattice require an Euclidean formulation of the theory, so the real time definition in Eq. 1 can not be directly employed. Different strategies can be adopted, and most of them are based on the fact that $\Gamma_{\rm Sphal}$ is related to the *spectral density* $\rho(\omega)$ of the Euclidean topological charge density time correlator $G(t)$ via the *Kubo formula* (T is the temperature)

$$\Gamma_{\rm Sphal} = 2T \lim_{\omega\to 0} \frac{\rho(\omega)}{\omega}. \tag{3}$$

More precisely, the quantity directly accessible on the lattice is the Euclidean time correlator of the topological charge density operator $G(t)$, related to the spectral density $\rho(\omega)$ via the integral relation (now t is the imaginary time)

$$G(t) \equiv \int d^3x \langle q(t,\vec{x}) q(0,\vec{0}) \rangle = -\int_0^\infty \frac{d\omega}{\pi} \rho(\omega) \frac{\cosh\left[\frac{\omega}{2T} - \omega t\right]}{\sinh\left[\frac{\omega}{2T}\right]}. \tag{4}$$

The strategy is now clear: firstly, one can determine $G(t)$ from lattice simulations and then invert Eq. 4 to obtain $\Gamma_{\rm Sphal}$. However, this kind of inversion is a very complicated task, being a mathematical ill-posed problem[1].

Different approaches have been developed to attack this kind of problem [3, 8–20]. Among them, we adopt the well-known Hansen–Lupo–Tantalo (HLT) [17] modification of the Backus–Gilbert method [14], which allows to estimate the $g_t(0)$ coefficients and finally write the spectral

[1] We refer the reader to Refs. [6, 7] for some recent reviews on the topic.

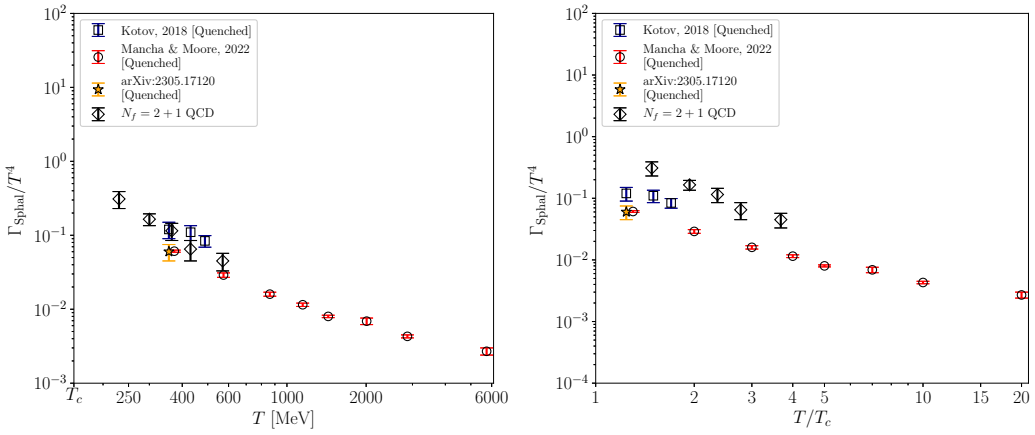

Figure 1: $N_f = 2+1$ *QCD sphaleron rate behaviour, represented with diamond points taken from Ref. [24], as a function of the temperature. A comparison with some previous quenched results is also done: square points are taken from Refs. [21, 22], round markers from Ref. [23] and, finally, the starred one from Ref. [25]. Left: x-axis expressed in terms of the absolute temperature in* MeV. *Right: x-axis expressed in terms of* T/T_c*, with* $T_c = 155$ MeV *and* $T_c = 287$ MeV *for full QCD and the quenched theory, respectively.*

density as a linear combination of the correlator at different times

$$\frac{\Gamma_{\rm Sphal}}{2T} = \left[\frac{\bar{\rho}(\bar{\omega})}{\bar{\omega}}\right]_{\bar{\omega}=0} = -\pi \sum_{t=0}^{1/T} g_t(0) G(t). \tag{5}$$

In the literature only few attempts for the computation of $\Gamma_{\rm Sphal}$ are reported, and most of them regard the quenched theory [21–23]. The QCD case, the relevant one for the axion phenomenology, has recently been investigated for the first time [24] for 5 different temperatures in the range 200 MeV $\lesssim T \lesssim$ 600 MeV by adopting a methodology already tested in the quenched case [25], which turned out to be consistent with the previous determinations in the literature. A summary of the QCD results, and a comparison with the quenched determinations, can be found in Fig. 1.

In this talk, we focus on the extension of the sphaleron rate computation to the non-zero spatial momentum case that is relevant for axion phenomenology. First of all, following Ref. [5], we motivate this kind of study. Then, after discussing the numerical setup, we show some very preliminary results for the quenched theory. Finally, we conclude with some comments and future outlooks.

2. Axion rate from strong sphalerons

The axion distribution function $f_{\vec{p}}$ with comoving 3-momentum $\vec{p}$ in the QCD thermal bath can be obtained by solving the Boltzmann equation

$$\frac{df_{\vec{p}}}{dt} = (1 + f_{\vec{p}})\Gamma^{<} - f_{\vec{p}}\Gamma^{>}\,, \tag{6}$$

where the axion is assumed to have a negligible mass (so $p^\mu = (E = |\vec{p}|, \vec{p})$), while $\Gamma^{<}$ and $\Gamma^{>}$ describe the energy dependent creation/destruction rates. At the thermal equilibrium in the QCD

bath, the following non-perturbative relation holds

$$\Gamma^{>} = \exp\left(\frac{E}{T}\right)\Gamma^{<} = \frac{\Gamma^{>}_{\rm top}}{2E f_a^2}\,, \tag{7}$$

where T is the temperature and $\Gamma^{>}_{\rm top}$ is the *topological rate* related to the 2-point correlation function of the topological charge density operator $q(x)$

$$\Gamma^{>}_{\rm top}(p^\mu) \equiv \int d^4x\, e^{ip^\mu x_\mu}\langle q(x^\mu)q(0)\rangle\,. \tag{8}$$

It is worth noticing that $\Gamma^{>}_{\rm top}(p^\mu = 0) = \Gamma_{\rm Sphal}$ (compare with Eq. 1).

It is now clear the motivation of the extension of the sphaleron rate computation to the non-zero momentum case: what is really needed to put more stringent bounds on the axion mass is the 3-momentum dependence of $\Gamma^{>}_{\rm top}(\vec{p})$, i.e., the *total* axion production rate. Moreover, the authors of Ref. [5] also argue that for $T \lesssim 5$ GeV the contribution to $\Gamma^{>}_{\rm top}(\vec{p})$ is dominated by sphalerons. This is the reason why the topological rate is expected to be constant for values of 3-momenta $|\vec{p}|$ smaller that the 3-momentum associated to the sphaleron size $|\vec{p}_s| \sim N_c\alpha_s T$

$$\Gamma^{>}_{\rm top}(E = |\vec{p}| \lesssim |\vec{p}_s|) \simeq \Gamma^{>}_{\rm top}(E = 0) \equiv \Gamma_{\rm Sphal}, \tag{9}$$

while it is expected to sharply decay for $|\vec{p}| \gtrsim |\vec{p}_s|$.

However, in order to determine explicitly the dependence of the topological rate on the 3-momentum, a very useful tool is provided by lattice QCD simulations. The approach is quite similar to the one sketched in Sec. 1. On the lattice, one can access the spatial Fourier transform of the Euclidean time-correlator of the topological charge density operator $G^{\vec{p}}(t)$, that can be expressed in terms of the spectral density $\rho(\omega, \vec{p})$ via the following integral relation

$$G^{\vec{p}}(t) \equiv \int d^3x\, e^{i\vec{p}\cdot\vec{x}}\langle q(t,\vec{x})q(0,\vec{0})\rangle = -\int \frac{d\omega}{\pi}\rho(\omega,\vec{p})\frac{\cosh\left[\frac{\omega}{2T} - \omega t\right]}{\sinh\left[\frac{\omega}{2T}\right]}. \tag{10}$$

Once $G^{\vec{p}}(t)$ has been computed on the lattice, one can rely on the Kubo formula for the non-zero momentum case, invert the correlator via the HLT Backus–Gilbert and obtain the non-zero momentum topological rate [26]

$$\Gamma^{>}_{\rm top}(|\vec{p}|) = \left[\coth\left(\frac{\bar{\omega}}{2T}\right)\bar{\rho}(\bar{\omega},\vec{p})\right]_{\bar{\omega}=|\vec{p}|} = \coth\left(\frac{|\vec{p}|}{2T}\right)\left[-\pi\sum_{t=0}^{1/T} g_t(\bar{\omega} = |\vec{p}|)G^{\vec{p}}(t)\right], \tag{11}$$

where the inversion now has to be performed in $\omega = |\vec{p}|$ because of the axion dispersion relation in the massless approximation. It is worth noticing that Eq. 11 reduces to Eq. 3 in the limit $\omega \to 0$, being $\coth(x) \sim 1/x$ for $x \to 0$.

3. Numerical results

In the following, we will show some preliminary results about the 3-momentum dependence of $G^{\vec{p}}(t)$ in the quenched case at $T \simeq 1.24\,T_c$ (the same of Refs. [21, 25]).

N_s	N_t	β	a [fm]	L [fm]	T/T_c
56	14	6.559	0.03948(58)	2.211(32)	1.242(18)
64	16	6.665	0.03450(50)	2.208(32)	1.244(18)
80	20	6.836	0.02759(40)	2.207(32)	1.244(18)

Table 1: *Summary of simulation parameters for the quenched case. For more details about the scale setting, we refer the reader to Ref. [25]. Scale setting obtained by interpolating results for a/r_0 of Ref. [31], where $r_0 = 0.472(5)$ fm [32] is the Sommer scale.*

We perform Monte Carlo simulations of the SU(3) gauge theory at $T \simeq 1.24\ T_c$, with $T_c \simeq 287$ MeV. We adopt the same lattice setup of Ref. [25]: the gauge sector is discretized with the standard Wilson action on $N_s^3 \times N_t$ lattices, and each Monte Carlo step consists of 1 lattice sweep of Over-Heat-Bath [27, 28] followed by 4 sweeps of Over-Relaxation [29], both implemented *à la* Cabibbo–Marinari [30]. The lattice parameters, summarized in Tab. 1, are the same of Ref. [25], with the exception that for this study we adopt a larger aspect ratio $N_s/N_t = 4$, to have a finer spacing among discretized lattice momenta.

The topological charge density operator is discretized with the standard clover definition, which has a definite parity

$$q_L(n_t;\vec{n}) = \frac{-1}{2^9\pi^2} \sum_{\mu\nu\rho\sigma=\pm1}^{\pm4} \varepsilon_{\mu\nu\rho\sigma} \mathrm{Tr}\{\Pi_{\mu\nu}(n_t;\vec{n})\Pi_{\rho\sigma}(n_t;\vec{n})\}, \tag{12}$$

where $\Pi_{\mu\nu}(n_t;\vec{n})$ is the plaquette starting from $n \equiv (n_t,\vec{n})$ and extending in the $\mu-\nu$ plane, and $\varepsilon_{(-\mu)\nu\rho\sigma} = -\varepsilon_{\mu\nu\rho\sigma}$. In order to compute $G^{\vec{p}}(t)$ on the lattice, it is useful to define the 3-momentum dependent time profile $Q_L^{\vec{p}}(n_t)$

$$Q_L^{\vec{p}}(n_t) \equiv \sum_{\vec{n}} e^{i\vec{p}\cdot\vec{n}} q_L(n_t;\vec{n}), \qquad \vec{p} = \frac{2\pi}{N_s}(k_x,k_y,k_z) \text{ with } k_i \in [0,\dots,N_s-1], \tag{13}$$

that allows us to easily determine the dimensionless spatial Fourier transform

$$\frac{G_L^{\vec{p}}(tT)}{T^5} = \frac{N_t^5}{N_s^3}\left\langle Q_L^{\vec{p}}(n_{t,1}) Q_L^{-\vec{p}}(n_{t,2})\right\rangle, \quad tT = \min\left\{\frac{|n_{t,1}-n_{t,2}|}{N_t}; 1-\frac{|n_{t,1}-n_{t,2}|}{N_t}\right\}, \tag{14}$$

where the normalized time separation tT is defined taking into account the presence of periodic boundary conditions.

Let us comment a little bit more on the choice of the external 3-momentum. Since there is not any source of anisotropy, we can choose without loss of generality a 3-momentum $\vec{p}$ oriented along a certain axis: indeed, the relevant quantity is $|\vec{p}|/T$. For our study we set $k \equiv k_x \neq 0$ and $k_y = k_z = 0$, i.e., $\vec{p}$ is oriented along the x-axis. However, in the future we are planning to take measurements also for momenta oriented in the y- and z-axis, in order to have a larger statistics.

The two-point function of the topological charge density operator is known to be affected by short distance singularities that give rise to an additive renormalization term [33, 34] that overcomes the physical signal in the continuum limit. In order to suppress these UV fluctuations, a smoothing

procedure is required. In this study we adopt cooling [35–41], characterized by a certain number $n_{\rm cool}$ of discrete steps, which can be associated to a *smearing radius* $r_s T \sim \sqrt{(8/3)n_{\rm cool}}/N_t$ [42]. The correlator is finally computed by performing a continuum limit at fixed smoothing radius r_s in physical units, followed by a zero smoothing limit. This is done according to a well-established procedure in the literature, and for more details we refer the reader to Refs. [25, 43].

For every value of k, or equivalently $|\vec{p}|/T$, the continuum limit is performed by assuming standard $O(1/N_t^2)$ corrections

$$\frac{G_L^{\vec{p}}\left(tT, N_t, \frac{n_{\rm cool}}{N_t^2}\right)}{T^5} = \frac{G^{\vec{p}}\left(tT, \frac{n_{\rm cool}}{N_t^2}\right)}{T^5} + b^{\vec{p}}\left(tT, \frac{n_{\rm cool}}{N_t^2}\right)\frac{1}{N_t^2} + o\left(\frac{1}{N_t^2}\right), \tag{15}$$

where it has been pointed out the fact that $O(1/N_t^2)$ corrections can in principle depend on the time separation tT, the smoothing radius and the 3-momentum $\vec{p}$. In Fig. 2, we display an example of continuum limit for $tT = 0.5$ and two different values of k: $k = 2, 4$, corresponding to $|\vec{p}|/T \simeq 3.14, 6.28$, respectively. It is clearly visible how our data are well described by the fit function in Eq. 15. The same conclusion still holds for other values of k and tT.

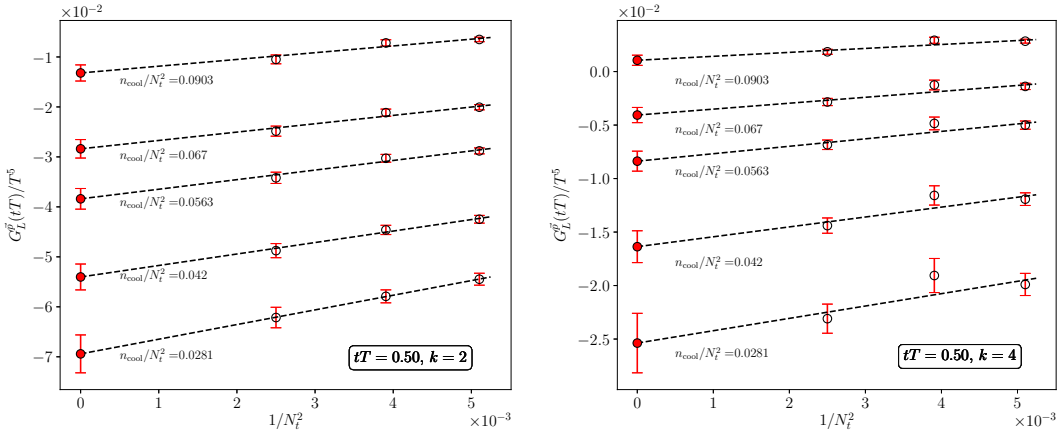

Figure 2: *Continuum limit of the correlator* $G_L^{\vec{p}}(tT)$*, at* $tT = 0.5$*, for some values of the smoothing radius* $(r_s T)^2 \propto n_{\rm cool}/N_t^2$*, according to the fit function in Eq. 15. Left:* $k = 2$*. Right:* $k = 4$*.*

Once the continuum limit has been performed, the correlator is affected by a residual dependence on the smoothing radius r_s, which has to be removed by performing a zero smoothing limit. According to what has been previously done in Refs. [25, 43], we assume linear corrections in $n_{\rm cool}/N_t^2$.

$$\frac{G^{\vec{p}}\left(tT, \frac{n_{\rm cool}}{N_t^2}\right)}{T^5} = \frac{G^{\vec{p}}(tT)}{T^5} + c^{\vec{p}}(tT)\frac{n_{\rm cool}}{N_t^2}. \tag{16}$$

When performing the $r_s \to 0$ limit, one has to pay attention to the fit range adopted[2]. More precisely, one has to perform a sufficient amount of smoothing to correctly identify the topological

[2]We refer the reader to Refs. [25, 43] for detailed discussions about this issue, since in this study we adopt the same criteria.

background. This criterium allows us to determine a lower bound for the fit range: in particular, we look for a common value $n_{\rm cool}^{(\rm min)}/N_t^2$ across all ensembles, where the topological susceptibility starts exhibiting a plateau. In this study we have $n_{\rm cool}^{(\rm min)}/N_t^2 \simeq 0.012$, the same value of Ref. [25]. With respect to the upper bound $n_{\rm cool}^{(\rm max)}/N_t^2$, we adopt the requirement for r_s not to be larger than the time separation tT, in order not to have overlapping sources in the correlator that would lead to unphysical results. As it can be appreciated from le left hand side plot of Fig. 3, where some examples of zero smoothing extrapolations are shown, Eq. 16 well describes our data. However, it is worth noticing that, when k becomes larger, the upper bound in the fit range gets smaller, i.e., deviations from linearity occur for smaller values of $n_{\rm cool}$.

In the right hand side plot of Fig. 3, the final result, i.e., the double extrapolated correlator $G^{\vec{p}}(tT)/T^5$, is shown for different values of $|\vec{p}|/T$. First of all, the double extrapolated correlator is negative for every $tT > 0$, as it should be according to the reflection positivity property [44]. As $|\vec{p}|/T$ is increased, the correlator is suppressed, signalling the fact that $\Gamma^{>}_{\rm top}(|\vec{p}|)$ decays. In particular, we have a significant suppression for $|\vec{p}|/T \simeq O(10)$.

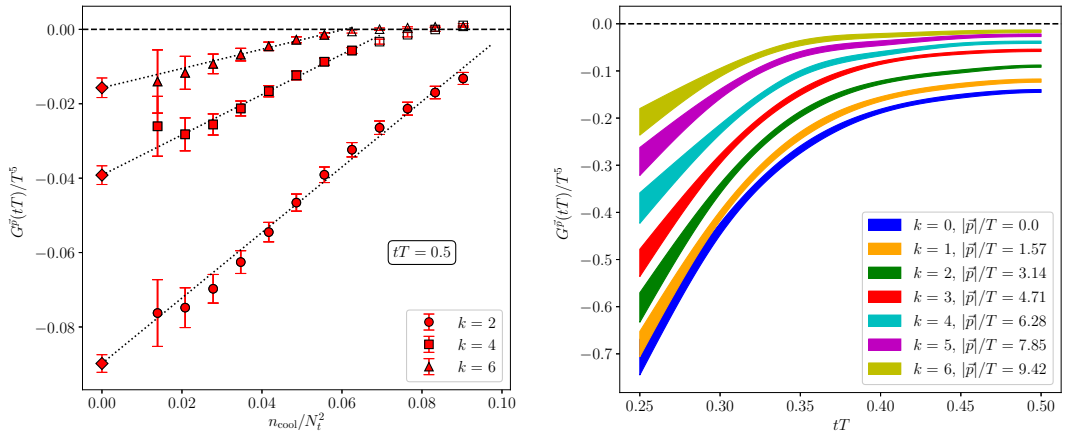

Figure 3: *Left: zero smoothing limit of $G^{\vec{p}}(tT, n_{\rm cool}/N_t^2)/T^5$ at $tT = 0.5$, for different values of k. A fit has been performed according to Eq. 16 using only filled points. A reference line in zero is also displayed. Right: double extrapolated correlator $G^{\vec{p}}(tT)/T^5$ as a function of $|\vec{p}|/T$, with a reference line in zero displayed.*

4. Conclusions and future outlooks

In this talk we presented the computation of the spatial Fourier transform of the two-point correlation function of the topological charge density operator by means of a double extrapolation procedure. This has been done for the pure SU(3) gauge theory at $T \simeq 1.24\ T_c$. We observe a suppression of the correlator as the 3-momentum $|\vec{p}|/T$ is increased: this suggests a decreasing behaviour of $\Gamma^{>}_{\rm top}(\vec{p})$ for large momenta, according to the results of Ref. [5].

We are planning to perform the inversion of the correlator in order to establish the shape of the topological rate as a function of the axion 3-momentum. In the future we will extend the computation of the topological rate to the full QCD case, at the same temperatures studied in Ref. [24]. This is necessary not only to put better constraints on the QCD axion phenomenology, but also to provide new insights on the structure of the QCD vacuum.

Acknowledgements

We thank G. Villadoro for useful discussions. The work of C. Bonanno is supported by the Spanish Research Agency (Agencia Estatal de Investigación) through the grant IFT Centro de Excelencia Severo Ochoa CEX2020-001007-S and, partially, by the grant PID2021-127526NB-I00, both of which are funded by MCIN/AEI/10.13039/501100011033. Numerical simulations have been performed on the `Leonardo` machine at Cineca, based on the agreement between INFN and Cineca, under project INF24_npqcd. This work has also been partially supported by the project "Non-perturbative aspects of fundamental interactions, in the Standard Model and beyond" funded by MUR, Progetti di Ricerca di Rilevante Interesse Nazionale (PRIN), Bando 2022, grant 2022TJFCYB (CUP I53D23001440006).

References

[1] K. Fukushima, D. E. Kharzeev and H. J. Warringa, *The Chiral Magnetic Effect*, *Phys. Rev. D* **78** (2008) 074033 [0808.3382].

[2] D. E. Kharzeev, *The Chiral Magnetic Effect and Anomaly-Induced Transport*, *Prog. Part. Nucl. Phys.* **75** (2014) 133 [1312.3348].

[3] N. Astrakhantsev, V. V. Braguta, M. D'Elia, A. Y. Kotov, A. A. Nikolaev and F. Sanfilippo, *Lattice study of the electromagnetic conductivity of the quark-gluon plasma in an external magnetic field*, *Phys. Rev. D* **102** (2020) 054516 [1910.08516].

[4] G. Almirante, N. Astrakhantsev, V. V. Braguta, M. D'Elia, L. Maio, M. Naviglio et al., *Electrical conductivity of the Quark-Gluon Plasma in the presence of strong magnetic fields*, 2406.18504.

[5] A. Notari, F. Rompineve and G. Villadoro, *Improved Hot Dark Matter Bound on the QCD Axion*, *Phys. Rev. Lett.* **131** (2023) 011004 [2211.03799].

[6] A. Rothkopf, *Inverse problems, real-time dynamics and lattice simulations*, *EPJ Web Conf.* **274** (2022) 01004 [2211.10680].

[7] G. Aarts et al., *Phase Transitions in Particle Physics - Results and Perspectives from Lattice Quantum Chromo-Dynamics*, *Prog. Part. Nucl. Phys.* **133** (2023) 104070 [2301.04382].

[8] D. Boito, M. Golterman, K. Maltman and S. Peris, *Spectral-weight sum rules for the hadronic vacuum polarization*, *Phys. Rev. D* **107** (2023) 034512 [2210.13677].

[9] J. Horak, J. M. Pawlowski, J. Rodríguez-Quintero, J. Turnwald, J. M. Urban, N. Wink et al., *Reconstructing QCD spectral functions with Gaussian processes*, *Phys. Rev. D* **105** (2022) 036014 [2107.13464].

[10] L. Del Debbio, T. Giani and M. Wilson, *Bayesian approach to inverse problems: an application to NNPDF closure testing*, *Eur. Phys. J. C* **82** (2022) 330 [2111.05787].

[11] A. Candido, L. Del Debbio, T. Giani and G. Petrillo, *Inverse Problems in PDF determinations*, *PoS* **LATTICE2022** (2023) 098 [2302.14731].

[12] A. Tikhonov, *Solution of Incorrectly Formulated Problems and the Regularization Method*, *Soviet Math. Dokl.* **4** (1963) 1035.

[13] N. Y. Astrakhantsev, V. V. Braguta and A. Y. Kotov, *Temperature dependence of the bulk viscosity within lattice simulation of SU(3) gluodynamics*, *Phys. Rev. D* **98** (2018) 054515 [1804.02382].

[14] G. Backus and F. Gilbert, *The Resolving Power of Gross Earth Data*, *Geophysical Journal International* **16** (1968) 169.

[15] B. B. Brandt, A. Francis, B. Jäger and H. B. Meyer, *Charge transport and vector meson dissociation across the thermal phase transition in lattice QCD with two light quark flavors*, *Phys. Rev. D* **93** (2016) 054510 [1512.07249].

[16] B. B. Brandt, A. Francis, H. B. Meyer and D. Robaina, *Pion quasiparticle in the low-temperature phase of QCD*, *Phys. Rev. D* **92** (2015) 094510 [1506.05732].

[17] M. Hansen, A. Lupo and N. Tantalo, *Extraction of spectral densities from lattice correlators*, *Phys. Rev. D* **99** (2019) 094508 [1903.06476].

[18] Extended Twisted Mass Collaboration (ETMC) collaboration, C. Alexandrou et al., *Probing the Energy-Smeared R Ratio Using Lattice QCD*, *Phys. Rev. Lett.* **130** (2023) 241901 [2212.08467].

[19] R. Frezzotti, N. Tantalo, G. Gagliardi, F. Sanfilippo, S. Simula and V. Lubicz, *Spectral-function determination of complex electroweak amplitudes with lattice QCD*, *Phys. Rev. D* **108** (2023) 074510 [2306.07228].

[20] Extended Twisted Mass collaboration, A. Evangelista, R. Frezzotti, N. Tantalo, G. Gagliardi, F. Sanfilippo, S. Simula et al., *Inclusive hadronic decay rate of the τ lepton from lattice QCD*, *Phys. Rev. D* **108** (2023) 074513 [2308.03125].

[21] A. Y. Kotov, *Sphaleron Transition Rate in Lattice Gluodynamics*, *JETP Letters* **108** (2018) 352.

[22] A. Y. Kotov, *Sphaleron rate in lattice gluodynamics*, *PoS* **Confinement2018** (2019) 147.

[23] M. Barroso Mancha and G. D. Moore, *The sphaleron rate from 4D Euclidean lattices*, *JHEP* **01** (2023) 155 [2210.05507].

[24] C. Bonanno, F. D'Angelo, M. D'Elia, L. Maio and M. Naviglio, *Sphaleron Rate of Nf=2+1 QCD*, *Phys. Rev. Lett.* **132** (2024) 051903 [2308.01287].

[25] C. Bonanno, F. D'Angelo, M. D'Elia, L. Maio and M. Naviglio, *Sphaleron rate from a modified Backus-Gilbert inversion method*, *Phys. Rev. D* **108** (2023) 074515 [2305.17120].

[26] D. T. Son and A. O. Starinets, *Minkowski space correlators in AdS / CFT correspondence: Recipe and applications*, *JHEP* **09** (2002) 042 [hep-th/0205051].

[27] M. Creutz, *Monte Carlo Study of Quantized $SU(2)$ Gauge Theory*, *Phys. Rev. D* **21** (1980) 2308.

[28] A. D. Kennedy and B. J. Pendleton, *Improved Heat Bath Method for Monte Carlo Calculations in Lattice Gauge Theories*, *Phys. Lett. B* **156** (1985) 393.

[29] M. Creutz, *Overrelaxation and Monte Carlo Simulation*, *Phys. Rev. D* **36** (1987) 515.

[30] N. Cabibbo and E. Marinari, *A New Method for Updating $SU(N)$ Matrices in Computer Simulations of Gauge Theories*, *Phys. Lett. B* **119** (1982) 387.

[31] S. Necco and R. Sommer, *The N(f) = 0 heavy quark potential from short to intermediate distances*, *Nucl. Phys. B* **622** (2002) 328 [hep-lat/0108008].

[32] R. Sommer, *Scale setting in lattice QCD*, *PoS* **LATTICE2013** (2014) 015 [1401.3270].

[33] P. Di Vecchia, K. Fabricius, G. C. Rossi and G. Veneziano, *Preliminary Evidence for $U(1)_A$ Breaking in QCD from Lattice Calculations*, *Nucl. Phys. B* **192** (1981) 392.

[34] M. D'Elia, *Field theoretical approach to the study of theta dependence in Yang-Mills theories on the lattice*, *Nucl. Phys. B* **661** (2003) 139 [hep-lat/0302007].

[35] B. Berg, *Dislocations and Topological Background in the Lattice $O(3)$ σ Model*, *Phys. Lett. B* **104** (1981) 475.

[36] Y. Iwasaki and T. Yoshie, *Instantons and Topological Charge in Lattice Gauge Theory*, *Phys. Lett. B* **131** (1983) 159.

[37] S. Itoh, Y. Iwasaki and T. Yoshie, *Stability of Instantons on the Lattice and the Renormalized Trajectory*, *Phys. Lett. B* **147** (1984) 141.

[38] M. Teper, *Instantons in the Quantized $SU(2)$ Vacuum: A Lattice Monte Carlo Investigation*, *Phys. Lett. B* **162** (1985) 357.

[39] E.-M. Ilgenfritz, M. Laursen, G. Schierholz, M. Müller-Preussker and H. Schiller, *First Evidence for the Existence of Instantons in the Quantized $SU(2)$ Lattice Vacuum*, *Nucl. Phys. B* **268** (1986) 693.

[40] M. Campostrini, A. Di Giacomo and H. Panagopoulos, *The Topological Susceptibility on the Lattice*, *Phys. Lett. B* **212** (1988) 206.

[41] B. Alles, L. Cosmai, M. D'Elia and A. Papa, *Topology in $2D$ CP^{N-1} models on the lattice: A Critical comparison of different cooling techniques*, *Phys. Rev. D* **62** (2000) 094507 [hep-lat/0001027].

[42] C. Bonati and M. D'Elia, *Comparison of the gradient flow with cooling in $SU(3)$ pure gauge theory*, *Phys. Rev. D* **D89** (2014) 105005 [1401.2441].

[43] L. Altenkort, A. M. Eller, O. Kaczmarek, L. Mazur, G. D. Moore and H.-T. Shu, *Sphaleron rate from Euclidean lattice correlators: An exploration*, *Phys. Rev. D* **103** (2021) 114513 [2012.08279].

[44] E. Vicari, *The Euclidean two point correlation function of the topological charge density*, *Nucl. Phys. B* **554** (1999) 301 [hep-lat/9901008].